

## Synthesis, Characterization and Comparative Study of New Functionalized Imidazolium-Based Ionic Liquids Derivatives Towards Corrosion of C38 Steel in Molar Hydrochloric Acid

A.Zarrouk<sup>1, \*</sup>, M. Messali<sup>4</sup>, H. Zarrok<sup>2</sup>, R. Salghi<sup>3</sup>, A. Al-Sheikh Ali<sup>4</sup>, B. Hammouti<sup>1</sup>, S. S. Al-Deyab<sup>5</sup>, F. Bentiss<sup>6</sup>

<sup>1</sup> LCAE-URAC18, Faculté des Sciences, Université Mohammed 1<sup>er</sup>, Oujda, Morocco.

<sup>2</sup> Laboratoire des procédés de séparation, Faculté des Sciences, Université Ibn Tofail, Kénitra, Morocco.

<sup>3</sup> Equipe de Génie de l'Environnement et Biotechnologie, ENSA, Université Ibn Zohr, BP1136 Agadir, Morocco.

<sup>4</sup> Chemistry Department, Faculty of Science, Taibah University, 30002, Al-Madinah AlMounawara, Saudi Arabia

<sup>5</sup> Petrochemical Research Chair, Chemistry Department, College of Science, King Saud University, P.O. Box 2455, Riyadh 11451, Saudi Arabia.

<sup>6</sup> Laboratoire de Chimie de Coordination et d'Analytique (LCCA), Faculté des Sciences, Université Chouaib Doukkali, B.P. 20, M-24000 El Jadida, Morocco.

\*E-mail: [azarrouk@gmail.com](mailto:azarrouk@gmail.com)

Received: 20 June 2012 / Accepted: 9 July 2012 / Published: 1 August 2012

---

This study examines the use of new imidazolium-based ionic liquids derivatives, namely 3-(3-phenylpropyl)-1-propyl-1H-imidazol-3-ium bromide (PPIB1) and 3-(4-phenoxybutyl)-1-propyl-1H-imidazol-3-ium bromide (PPIB4) for corrosion and dissolution protection of C38 steel in normal hydrochloric acid solution. The inhibiting efficiency of the different additives was evaluated by means of weight loss and electrochemical techniques such as AC impedance measurements and polarization curves. The experimental results obtained reveal that PPIB4 was the most effective inhibitor. The variation in inhibitive efficiency mainly depends on the type and nature of the substituents present in the inhibitor molecule. Polarization curves showed that the new imidazolium ionic liquids were mixed-type inhibitors in 1 M HCl. The inhibition efficiency increased with imidazolium ionic liquids concentration and attained the maximum value of 94.2% in the case of PPIB4 at  $10^{-2}$  M. The results obtained from weight loss and electrochemical studies were in reasonable agreement. The adsorption of PPIB1 and PPIB4 on the steel surface obeyed to the Langmuir isotherm model. The thermodynamic data of activation were determined and discussed.

---

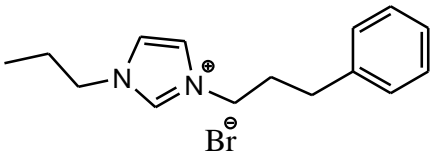
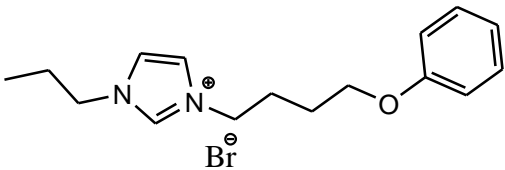
**Keywords:** Steel, Hydrochloric acid, imidazolium ionic liquids, Polarization curves, EIS.

## 1. INTRODUCTION

Acid solutions are, especially hydrochloric acid, widely used in various industrial processes such as oil well acidification, the petrochemical processes, acid pickling and acidic cleaning [1–3], which generally leads to serious metallic corrosion. As the most effective and economic method, inhibitors are applied in these acid solutions to control the metal dissolution [4, 5]. There is a considerable amount of effort devoted to develop novel and efficient corrosion inhibitors. Organic compounds usually serve as inhibitors, and generally protect the metal from corrosion by forming a protection film on the metal surface [6]. Most of the well-known organic inhibitors are the compounds containing nitrogen, sulfur, oxygen atoms and  $\pi$ -bonds [7-12].

Recently, Ionic liquids have been also widely investigated for a variety of applications [13–17]. In particular, the most extensively studied ILs is based upon the imidazolium cation. Imidazolium, pyridinium and pyridazinium-based ionic liquids are reported to show corrosion resistant behaviour on copper [18, 19] and mild steel [20-22]. It was found that the action of such inhibitors depends on the specific interaction between the functional groups and the metal surface, due to the presence of the  $C=N$ - group and electronegative nitrogen in the molecule.

In this work, we have synthesized a variety of new N-alkylimidazolium ionic liquids namely, 3-(3-phenylpropyl)-1-propyl-1H-imidazol-3-ium bromide (PPIB1) and 3-(4-phenoxybutyl)-1-propyl-1H-imidazol-3-ium bromide (PPIB4), with the aim to study their applicability as corrosion inhibitors for carbon steel in 1.0 M HCl by weight loss, AC impedance and polarization techniques were employed for this purpose. The effect of concentration and temperature on the inhibition efficiency has been examined. The thermodynamic parameters for dissolution processes were calculated and discussed. The chemical structures of the studied imidazolium ionic liquids are given in Fig 1.

Abbreviation	Structural formula	Name
PPIB1		3-(3-phenylpropyl)-1-propyl-1H-imidazol-3-ium bromide
PPIB4		3-(4-phenoxybutyl)-1-propyl-1H-imidazol-3-ium bromide

**Figure 1.** The chemical structure of the studied imidazolium ionic liquids.

## 2. EXPERIMENTAL METHODS

### 2.1. Materials

The steel used in this study is a carbon steel (Euronorm: C35E carbon steel and US specification: SAE 1035) with a chemical composition (in wt%) of 0.370 % C, 0.230 % Si, 0.680 % Mn, 0.016 % S, 0.077 % Cr, 0.011 % Ti, 0.059 % Ni, 0.009 % Co, 0.160 % Cu and the remainder iron (Fe). The carbon steel samples were pre-treated prior to the experiments by grinding with emery paper SiC (120, 600 and 1200); rinsed with distilled water, degreased in acetone in an ultrasonic bath immersion for 5 min, washed again with bidistilled water and then dried at room temperature before use. The acid solutions (1 M HCl) were prepared by dilution of an analytical reagent grade 37 % HCl with double-distilled water. The concentration range of PPIB1 and PPIB4 employed was  $10^{-5}$  M to  $10^{-2}$  M.

### 2.2. Synthesis

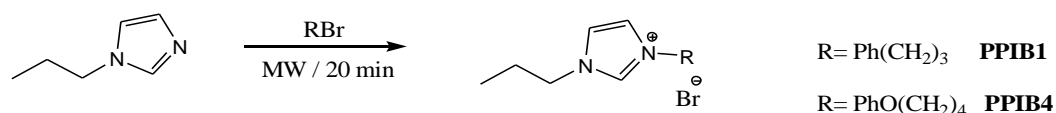
#### 2.2.1. Measurements and equipments

All synthesized compounds were and characterized using  $^1\text{H}$  NMR (400 MHz) and  $^{13}\text{C}$  NMR (100 MHz) spectroscopies. The spectra were obtained in DMSO at room temperature. Chemical shifts ( $\delta$ ) were reported in ppm to a scale calibrated for tetramethylsilane (TMS) as an internal standard. The LC-MS spectra were measured using a Micromass, LCT mass spectrometer. The microwave-assisted reactions were performed using a controllable single-mode microwave reactor, CEM Discovery, designed for synthetic use. The reactor is equipped with a magnetic stirrer as well as a pressure, temperature and power controls. The maximum operating pressure of the reactor is 20 bar. The power and temperature range are 15 - 300 W and 60 – 250 °C, respectively.

#### 2.2.2. Microwave assisted synthesis of imidazolium-based ionic liquids

Many procedures are recommended for the Green Chemistry [23] involving: solvent-free reactions, non-classical modes of activation such as ultrasounds or microwaves. The use of MW irradiation leads to large reductions in reaction times, enhancements in conversions, sometimes in selectivity, with several advantages of the eco-friendly approach [24-27].

In continuation of our previous works, new environmentally friendly imidazolium-based ionic liquids (PPIB1 and PPIB4) were prepared using microwave irradiation in short duration of time with quantitative yields [28, 29].



**Scheme 1.** Synthesis of new imidazolium-based ionic liquids under microwave irradiation (MW).

The nucleophilic alkylation of 1-propylimidazole with different functionalized alkyl halides afforded the corresponding imidazolium ionic liquids in 85-88% yield. (Table1)

**Table 1.** Different entries and reaction yields for the synthesis of imidazolium-based ionic liquids under microwave irradiation (MW).

Entry	RX	Yield (%)
PPIB1	Ph(CH <sub>2</sub> ) <sub>3</sub>	85
PPIB4	PhO(CH <sub>2</sub> ) <sub>4</sub> Br	88

### 2.2.2.1 synthesis of 3-(3-phenylpropyl)-1-propyl-1H-imidazol-3-ium bromide (PPIB1)

1-propylimidazole (2g, 0.018 mol), (3-bromopropyl)benzene (3.98g, 0.02 mol) and 20 mL of toluene were placed in a microwave reactor vessel and irradiated for 20 minutes at 100°C. The crude product was washed a few times with dry ethyl acetate and dried overnight in a vacuum at 70 °C. The yield of PPIB1 was 85%. The product was analyzed using <sup>1</sup>H NMR, <sup>13</sup>C NMR and LCMS. <sup>1</sup>H NMR (400MHz, DMSO) δ: 0.81 (t, J = 7.6, 3H), 1.76 (quint, J = 7.6, 2H), 2.34 (quint, J = 7.2, 2H), 2.65 (t, J = 7.2, 2H), 4.02 (t, J = 7.6, 2H), 4.88 (t, J = 7.2, 2H), 7.28-7.34 (m, 5H), 7.93 (d, 1H), 7.96 (d, 1H), 9.98 (s, 1H); <sup>13</sup>C NMR (100MHz, DMSO) δ: 30.8 (CH<sub>2</sub>), 31.5 (CH<sub>2</sub>), 64.2 (CH<sub>2</sub>), 126.1 (CH), 128.2 (CH), 128.4 (CH), 135.9(CH), 136.5(CH), 140.1(C), 149.7 (CH), 154.2 (CH); LCMS: m/z 229 (M-Br) found for C<sub>15</sub>H<sub>21</sub>N<sub>2</sub><sup>+</sup>.

### 2.2.2.2 synthesis of 3-(4-phenoxybutyl)-1-propyl-1H-imidazol-3-ium bromide (PPIB4)

1-propylimidazole (2g, 0.018 mol), (4-bromobutoxy)benzene (4.52g, 0.02 mol) and 20mL of toluene were placed in a microwave reactor vessel and irradiated for 20 minutes at 100 °C. The crude product was washed a few times with dry ethyl acetate and dried overnight in a vacuum at 70 °C. The yield of PPIB4 was 88%. The product was analyzed with <sup>1</sup>H NMR, <sup>13</sup>C NMR and LCMS. <sup>1</sup>H NMR (400MHz, DMSO) δ: 0.94 (t, J = 7.6, 3H), 1.82 (quint, J = 7.6, 2H), 1.97 (quint, J = 7.6, 2H), 2.14 (quint, J = 7.6, 2H), 3.99 (t, J = 6.8, 2H), 4.27 (t, J = 7.6, 2H), 4.46 (t, J = 6.8, 2H), 6.85-6.93 (m, 3H), 7.23-7.27 (m, 2H), 7.63 (d, 1H), 7.70 (d, 1H), 10.30 (s,1H); <sup>13</sup>C NMR (100MHz, DMSO) δ: 10.17 (CH<sub>3</sub>), 23.0 (CH<sub>2</sub>), 25.3 (CH<sub>2</sub>), 26.8 (CH<sub>2</sub>), 49.0 (CH<sub>2</sub>), 50.8 (CH<sub>2</sub>), 66.2 (CH<sub>2</sub>), 113.8 (CH), 120.2 (CH), 121.9 (CH), 122.0(CH), 128.9(CH), 135.9(CH), 157.9(C); LCMS: m/z 259 (M-Br) found for C<sub>16</sub>H<sub>23</sub>N<sub>2</sub>O<sup>+</sup>;

## 2.3. Measurements

### 2.3.1. Weight loss measurements

The gravimetric measurements were carried out at definite time interval of 6 h at room temperature using an analytical balance (precision ± 0.1 mg). The carbon steel specimens used have a rectangular form (length = 1.6 cm, width = 1.6 cm, thickness = 0.07 cm). Gravimetric experiments

were carried out in a double glass cell equipped with a thermostated cooling condenser containing 50 mL of non-de-aerated test solution. After immersion period, the steel specimens were withdrawn, carefully rinsed with bidistilled water, ultrasonic cleaning in acetone, dried at room temperature and then weighted. Triplicate experiments were performed in each case and the mean value of the weight loss was calculated.

### 2.3.2. Electrochemical measurements

Electrochemical experiments were conducted using impedance equipment (Tacussel-Radiometer PGZ 100) and controlled with Tacussel corrosion analysis software model Voltmaster 4. A conventional three-electrode cylindrical Pyrex glass cell was used. The temperature is thermostatically controlled. The working electrode was carbon steel with the surface area of 1 cm<sup>2</sup>. A saturated calomel electrode (SCE) was used as a reference. All potentials were given with reference to this electrode. The counter electrode was a platinum plate of surface area of 1 cm<sup>2</sup>. A saturated calomel electrode (SCE) was used as the reference; a platinum electrode was used as the counter-electrode. All potentials are reported vs. SCE. All electrochemical tests have been performed in aerated solutions at 308 K.

For polarization curves, the working electrode was immersed in a test solution during 30 min until a steady state open circuit potential ( $E_{ocp}$ ) was obtained. The polarization curve was recorded by polarization from -600 to -300 mV/SCE with a scan rate of 1 mV s<sup>-1</sup>). AC impedance measurements were carried-out in the frequency range of 100 kHz to 10 mHz, with 10 points per decade, at the rest potential, after 30 min of acid immersion, by applying 10 mV ac voltage peak-to-peak. Nyquist plots were made from these experiments. The best semicircle can be fit through the data points in the Nyquist plot using a non-linear least square fit so as to give the intersections with the  $x$ -axis.

## 3. RESULTS AND DISCUSSION

### 3.1. Gravimetric study

#### 3.1.1. Effect of inhibitors concentration

The effect of addition of 3-(3-phenylpropyl)-1-propyl-1H-imidazol-3-ium bromide (PPIB1) and 3-(4-phenoxybutyl)-1-propyl-1H-imidazol-3-ium bromide (PPIB4) tested at different concentrations on the corrosion of C38 steel in 1.0 M HCl solution was studied by weight loss measurements at 308 K after 6 h of immersion period. The corrosion rate (CR) and inhibition efficiency  $\eta_{WL}(\%)$  were calculated according to the equations. 1 and 2 [30,31], respectively:

$$C_R = \frac{W_b - W_a}{At} \quad (1)$$

$$\eta_{WL}(\%) = \left(1 - \frac{w_i}{w_0}\right) \times 100 \tag{2}$$

where  $W_b$  and  $W_a$  are the specimen weight before and after immersion in the tested solution,  $w_0$  and  $w_i$  are the values of corrosion weight losses of carbon steel in uninhibited and inhibited solutions, respectively,  $A$  the total area of the carbon steel specimen ( $\text{cm}^2$ ) and  $t$  is the exposure time (h).

The values of percentage inhibition efficiency  $\eta_{WL}(\%)$  and corrosion rate (CR) obtained from weight loss method at different concentrations of PPIB1 and PPIB4 at 308 K are summarized in Table 2. It is very clear that the two compounds inhibits the corrosion of C38 steel in 1.0 M HCl solution, at all concentrations used in this study, and the corrosion rate (CR) decreases continuously with increasing additive concentration at 308 K. Indeed, corrosion rate values of C38 steel decrease when the inhibitor concentration increases while  $\eta_{WL}(\%)$  values of PPIB1 and PPIB4 increase with the increase of the concentration. In other words, their inhibition efficiency increased to reach the higher value of 92.3% for PPIB1 and 94.2% for PPIB4 at  $10^{-2}$  M. The plausible mechanism for corrosion inhibition of C38 steel in 1 M HCl by PPIB1 and PPIB4 may be explained on the basis of adsorption behavior. The adsorption of the imidazolium derivatives molecules on the metal surface is through the already adsorbed chloride ion. In acidic solutions, the imidazolium derivatives molecules exist as cations and adsorb through electrostatic interactions between the positively charged PPIB1 and PPIB4 cations and adsorbed chloride ions [32]. Owing to the acidity of the medium, imidazolium derivatives molecules can exist as a neutral species or in the cationic form. Thus, the adsorption of the neutral imidazolium derivatives molecules could occur due to the formation of links between the d orbital of iron atoms, involving the displacement of water molecules from the metal surface, and the lone sp<sup>2</sup> electron pairs present on the N and/or O atoms. The hydrophobic spacer ( $\text{CH}_2\text{-CH}_2$ ) in two compounds may act as an effective barrier from the aggressive medium. Moreover, the presence of electron pairs on the oxygen atom may be attributed to an increase in the electron density leading to electron transfer mechanism from PPIB4 to metal surface. Also, the larger molecular size of PPIB4 can be considered which ensures greater coverage of the metallic surface [33–35].

**Table 2.** Corrosion parameters obtained from weight loss measurements for carbon steel in 1.0 M HCl containing various concentrations of inhibitors at 308 K.

Inhibitors	Conc (M)	CR (mg/cm <sup>2</sup> h)	$\eta_{WL}(\%)$	$\theta$
Blank	1	1.070	-----	-----
PPIB1	$1 \times 10^{-5}$	0.373	65.1	0.651
	$1 \times 10^{-4}$	0.231	78.4	0.784
	$1 \times 10^{-3}$	0.158	85.2	0.852
	$5 \times 10^{-3}$	0.119	88.9	0.889
	$1 \times 10^{-2}$	0.082	92.3	0.923
PPIB4	$1 \times 10^{-5}$	0.316	70.5	0.705
	$1 \times 10^{-4}$	0.213	80.1	0.801
	$1 \times 10^{-3}$	0.147	86.3	0.863
	$5 \times 10^{-3}$	0.090	91.6	0.916
	$1 \times 10^{-2}$	0.062	94.2	0.942

### 3.1.2. Effect of temperature

The effect of temperature on the inhibited acid–metal reaction is very complex. Because many changes occur on the metal surface such as rapid etching desorption of inhibitor and the inhibitor itself may undergoes decomposition [36]. The change of the corrosion rate at selected concentrations of the PPIB1 and PPIB4 during 1 h of immersion with the temperature was studied in 1.0 M HCl both in absence and the presence of two compounds. For this purpose, gravimetric experiments were performed at different temperatures (308–343 K). The fractional surface coverage  $\theta$  can be easily determined from weight loss measurements by the ratio  $\eta_{WL}\% / 100$  if one assumes that the values of  $\eta_{WL}\%$  do not differ substantially from  $\theta$ . It is clear from Table 3 that increasing the corrosion rate ( $C_R$ ) was more pronounced with the rise of temperature for blank solution. In the presence of the PPIB1 and PPIB4 molecules, the corrosion rate of steel decreased at any given temperature as inhibitor concentration increased due to the increasing of the degree of surface coverage.

**Table 3.** Various corrosion parameters for carbon steel in 1.0 M HCl in the absence and the presence of optimum concentration of PPIB1 and PPIB4 at different temperatures after 1h.

Temp (K)	Inhibitors	$C_R$ (mg/cm <sup>2</sup> h)	$\eta_{WL}\%$	$\theta$
	Blank	1.070	-----	-----
308	PPIB1	0.082	92.3	0.923
	PPIB4	0.062	94.2	0.942
	Blank	1.49	-----	-----
313	PPIB1	0.171	88.5	0.885
	PPIB4	0.122	91.8	0.918
	Blank	2.870	-----	-----
323	PPIB1	0.502	82.5	0.825
	PPIB4	0.367	87.2	0.872
	Blank	5.210	-----	-----
333	PPIB1	1.454	72.1	0.721
	PPIB4	1.094	79.0	0.790
	Blank	10.02	-----	-----
343	PPIB1	4.028	59.8	0.598
	PPIB4	3.176	68.3	0.683

In contrast, at constant inhibitor concentration, the corrosion rate increased with increasing the temperature. Hence we noted that the efficiency depends on the temperature and decreased with the rise of temperature from 308 to 343 K. This can be explained by the decrease of the strength of the adsorption process at elevated temperature and would suggest a physical adsorption mode. To calculate the activation thermodynamic parameters of the corrosion process, Arrhenius Eq. (3) and transition state Eq. (4) were used [37]:

$$C_R = k \exp\left(-\frac{E_a}{RT}\right) \quad (3)$$

$$C_R = \frac{RT}{Nh} \exp\left(\frac{\Delta S_a}{R}\right) \exp\left(-\frac{\Delta H_a}{RT}\right) \quad (4)$$

Where  $E_a$  is the apparent activation corrosion energy;  $R$  is the universal gas constant;  $k$  is the Arrhenius pre-exponential factor.  $h$  is Plank's constant.  $N$  is Avogadro's number.  $\Delta S_a$  is the entropy of activation and  $\Delta H_a$  is the enthalpy of activation.

Arrhenius plots for the corrosion rate of C38 steel are given in Fig. 2. Values of apparent activation energy of corrosion ( $E_a$ ) for C38 steel in 1.0 M HCl with the absence and the presence of various concentrations of PPIB were determined from the slope of  $\ln(C_R)$  versus  $1/T$  plots PPIB1 and PPIB4 and shown in Table 4. The value of  $55.75 \text{ kJ mol}^{-1}$  obtained for the activation energy  $E_a$  of the corrosion process in 1.0 M HCl lies in the range of the most frequently cited values, the majority of which are grouped around  $60 \text{ kJ mol}^{-1}$  [38]. It was clear from this study that the values of  $A$  and  $E_a$  in the presence of PPIB1 and PPIB4 are higher than those of in the uninhibited acid solution. The experimental fact that the activation energy is higher in the presence of inhibitor was explained in different ways in the literature.

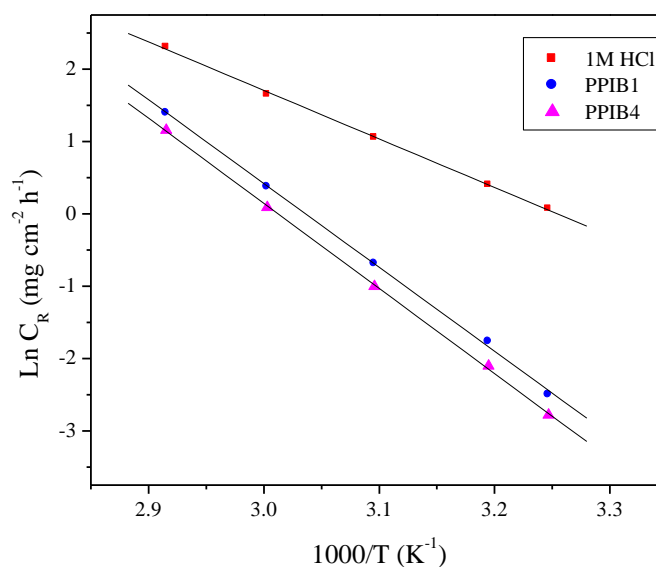


**Figure 2.** Arrhenius plots of  $\ln C_R$  vs.  $1/T$  for steel in 1.0 M HCl in the absence and the presence of PPIB1 and PPIB4 at optimum concentration.

According to Riggs and Hurd [38], the decrease in apparent activation energy at higher levels of inhibition arises from a shift of the net corrosion reaction, from one on the uncovered surface to one directly involving the adsorbed sites. This also reveals that the entire process is surface-reaction controlled, since the energy of activation for the corrosion process, both in the absence and the

presence of inhibitor, was greater than  $20 \text{ kJ mol}^{-1}$  [39]. Szauer and Brand explained that the increase in activation energy can be attributed to an appreciable decrease in the adsorption of the inhibitor on the C38 steel surface with increasing the temperature [40]. The increase in the activation energy after the addition of the inhibitor to the 1.0 M (out) HCl solution can indicate that physical adsorption (electrostatic) occurs in the first stage [41].

**Table 4.** Activation parameters for the steel dissolution in 1.0 M HCl in the absence and the presence of PPIB1 and PPIB4 at optimum concentration.

Inhibitors	A ( $\text{mg/cm}^2 \text{ h}$ )	Linear regression coefficient (r)	$E_a$ (kJ/mol)	$\Delta H_a$ (kJ/mol)	$\Delta S_a$ (J/mol K)
Blank	$3.0066 \times 10^9$	0.99961	55.75	53.05	-72.49
PPIB1	$1.9038 \times 10^{15}$	0.99954	96.34	93.64	38.57
PPIB4	$2.4696 \times 10^{15}$	0.99983	97.82	95.12	40.73

Fig. 3 showed a plot of  $\ln(C_R/T)$  versus  $1/T$ . The straight lines are obtained with a slope ( $\Delta H_a/R$ ) and an intercept of  $(\ln R/Nh + \Delta S_a/R)$  from which the values of the  $\Delta H_a$  and  $\Delta S_a$  are calculated and are (out) given in Table 4. Inspection of these data revealed that the thermodynamic parameters ( $\Delta H_a$  and  $\Delta S_a$ ) for dissolution reaction of steel in 1.0 M HCl in the presence of inhibitors is higher ( $93.64 \text{ kJ mol}^{-1}$  for PPIB1 and  $95.12 \text{ kJ mol}^{-1}$  for PPIB4) than that of in the absence of inhibitors ( $53.05 \text{ kJ mol}^{-1}$ ). The positive sign of  $\Delta H_a$  reflected the endothermic nature of the steel dissolution process suggesting that the dissolution of steel is slow [42] in the presence of inhibitor.

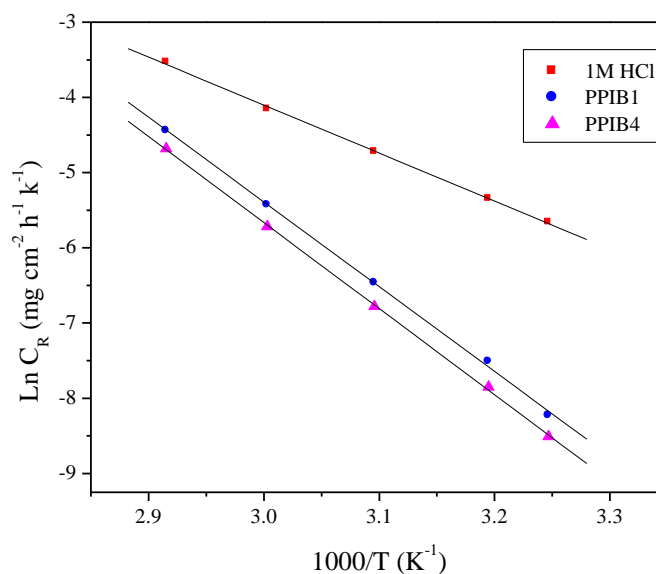


**Figure 3.** Arrhenius plots of  $\ln(C_R/T)$  vs.  $1/T$  for steel in 1.0 M HCl in the absence and the presence of PPIB1 and PPIB4 at optimum concentration.

The large negative value of  $\Delta S_a$  for C38 steel in 1.0 M HCl implies that the activated complex is the rate-determining step, rather than the dissociation step. In the presence of the inhibitors, the value of  $\Delta S_a$  increased and is generally interpreted as an increase in disorder as the reactants are converted to the activated complexes [43]. The positive values of  $\Delta S_a$  reflected the fact that the adsorption process is accompanied by an increase in entropy, which is the driving force for the adsorption of the inhibitor onto the steel surface.

### 3.1.3. Adsorption isotherm

In order to gain more information about the mode of adsorption of these compounds on the surface of carbon steel, the experimental data have been tested with several adsorption isotherms, including Langmuir, Frumkin, Freundlich and Temkin isotherms. However, the best fit was obtained from the Langmuir isotherm. Correlation between surface coverage ( $\theta$ ) defined by  $\eta_{WL}\% / 100$  and the concentration of inhibitor ( $C$ ) can be represented by the Langmuir adsorption isotherm, the isotherm is given by [44]:

$$\frac{C_{inh}}{\theta} = \frac{1}{K_{ads}} + C_{inh} \quad (5)$$

Where  $K_{ads}$  is the adsorption constant,  $C_{inh}$  is the concentration of the inhibitor and surface coverage values ( $\theta$ ) are obtained from the weight loss measurements for various concentrations.  $K_{ads}$  is the equilibrium constant of the adsorption process and is related to the standard Gibbs energy of adsorption,  $\Delta G_{ads}^{\circ}$ , according to [45]:

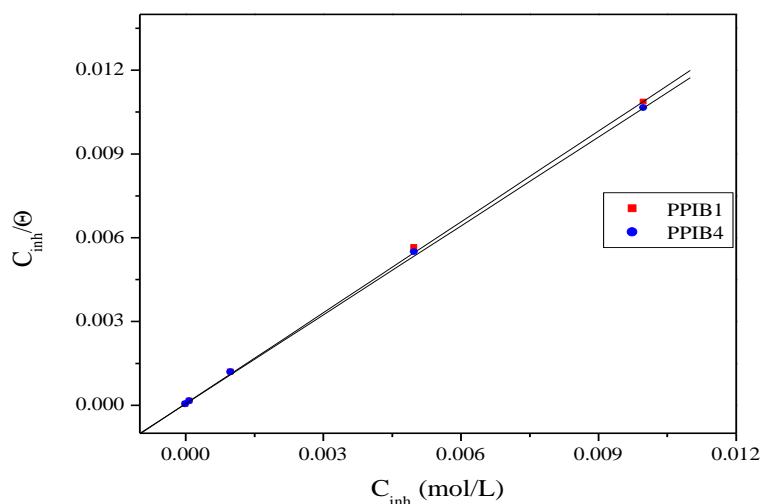
$$K_{ads} = \frac{1}{55.5} \exp\left(\frac{-\Delta G_{ads}^{\circ}}{RT}\right) \quad (6)$$

Where  $R$  is the universal gas constant and  $T$  is the absolute temperature. The value 55.5 in the above equation is the concentration of water in solution in mol/L.

Thermodynamic parameters are important to study the inhibitive mechanism. The values of  $K_{ads}$ ,  $R^2$  and  $\Delta G_{ads}^{\circ}$  are calculated and are (out) given in Table 5. The relation between  $C_{inh}/\theta$  and  $C_{inh}$  is shown in Fig. 4. These plots are linear with a slope equal to unity. This suggests that the adsorption of PPIB1 and PPIB4 on metal surface followed the Langmuir adsorption isotherm. This isotherm assumes that the adsorbed molecules occupy only one site and there are no interactions with other adsorbed species [46]. The correlation coefficient,  $R^2$ , was used to choose the isotherm that best fits the experimental data. The strong correlation ( $R^2 > 0.999$ ) suggests that the adsorption of inhibitor on the carbon steel surface obeyed this isotherm.

**Table 5.** Thermodynamic parameters for the adsorption of PPIB1 and PPIB4 in 1.0 M HCl on the C38 steel at 308K

Inhibitor	Slope	$K_{ads} (M^{-1})$	$R^2$	$\Delta G_{ads}^{\circ}$ (kJ/mol)
PPIB1	1.08	16615.2	0.99982	-35.17
PPIB4	1.06	18249.8	0.99989	-35.41

**Figure 4.** Langmuir adsorption of PPIB1 and PPIB4 on the steel surface in HCl solution

The value  $K_{ads}$  calculated from the reciprocal of intercept of isotherm line is indicating in Table 4. The high value of the adsorption equilibrium constant reflects the high adsorption ability of this inhibitor on C38 steel surface.

From Eq. (6),  $\Delta G_{ads}^{\circ}$  was calculated as  $-35.17 \text{ kJ mol}^{-1}$  for PPIB1 and  $-35.41 \text{ kJ mol}^{-1}$  for PPIB4. The negative value of standard free energy of adsorption indicates spontaneous adsorption of our molecules on C38 steel surface and also the strong interaction between inhibitor molecules and the metal surface [47, 48]. Generally, the standard free energy values of  $-20 \text{ kJ mol}^{-1}$  or less negative are associated with an electrostatic interaction between charged molecules and charged metal surface (physical adsorption); those of  $-40 \text{ kJ mol}^{-1}$  or more negative involves charge sharing or transfer from the inhibitor molecules to the metal surface to form a co-ordinate covalent bond (chemical adsorption) [49, 50]. Based on the literature [51], the calculated  $\Delta G_{ads}^{\circ}$  values in this work indicate that the adsorption mechanism of PPIB1 and PPIB4 on carbon steel in 1.0 M HCl solution at 308 K is both electrostatic-adsorption (ionic) and chemisorption (molecular) [52].

### 3.2. Tafel polarization study

Polarization measurements have been carried out in order to gain knowledge concerning the kinetics of the anodic and cathodic reactions. Typical potentiodynamic polarization curves of the

carbon steel in 1.0 M HCl solutions without and with addition of different concentrations of imidazolium ionic liquids are shown in Figs. 5 and 6. Electrochemical kinetic parameters (corrosion potential ( $E_{\text{corr}}$ ), corrosion current density ( $I_{\text{corr}}$ ) and cathodic Tafel slope ( $\beta_c$ )), determined from these experiments by extrapolation method [53], are reported in Table 6. The  $I_{\text{corr}}$  was determined by Tafel extrapolation of only the cathodic polarization curve alone, which usually produces a longer and better defined Tafel region [54]. The  $I_{\text{corr}}$  values were used to calculate the inhibition efficiency,  $\eta_{\text{Tafel}}(\%)$ , (listed in Table 6), using the following equation [55]:

$$\eta_{\text{Tafel}}(\%) = \frac{I_{\text{corr}} - I_{\text{corr}(i)}}{I_{\text{corr}}} \times 100 \quad (7)$$

Where  $I_{\text{corr}}$  and  $I_{\text{corr}(i)}$  are the corrosion current densities for steel electrode in the uninhibited and inhibited solutions, respectively. The parallel cathodic Tafel curves in Figs. 5 and 6 suggested that the hydrogen evolution was activation-controlled and the reduction mechanism was not affected by the presence of the inhibitor. The results in Table 6 showed that the inhibition efficiency increased, while the corrosion current density decreased with increasing imidazolium derivatives concentrations. This could be explained on the basis of adsorption of imidazolium derivatives on the carbon steel surface and the adsorption process enhanced with increasing inhibitor concentration.

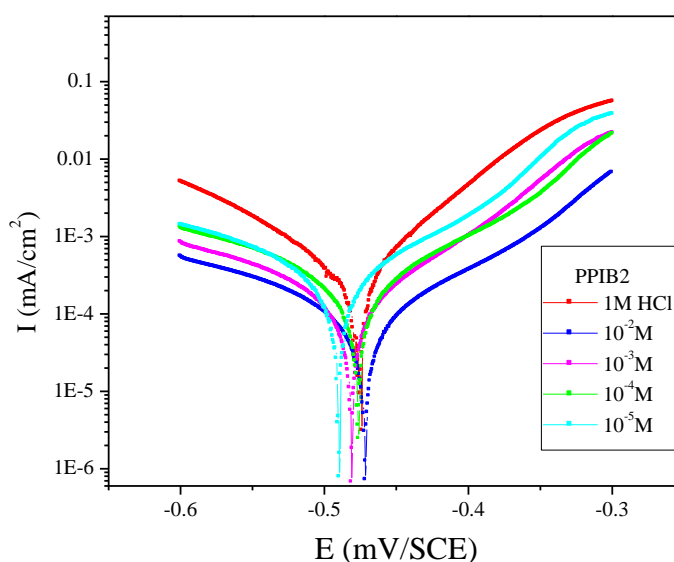


**Figure 5.** Polarisation curves of carbon steel in 1.0 M HCl for various concentrations of PPIB1.

The values of corrosion potential ( $E_{\text{corr}}$ ) were found to be almost identical at all imidazolium ionic liquids concentrations, indicating that it acts as mixed-type inhibitor [56]. From Table 5, it is clear that the values of cathodic Tafel slope constants were more or less constant suggesting that the presence of imidazolium derivatives molecules does not alter the mechanism of corrosion in HCl environment.

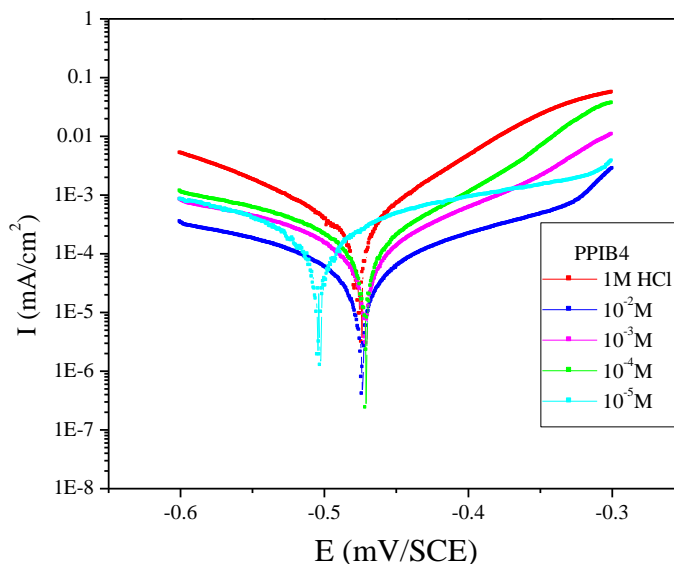


**Figure 6.** Polarisation curves of carbon steel in 1.0 M HCl for various concentrations of PPIB4.

**Table 6.** Polarization data of C38 steel in 1.0 M HCl without and with addition of inhibitor at 308 K.

Inhibitors	Concentration (M)	$-E_{corr}$ (mV/SCE)	$-\beta_c$ (mV dec <sup>-1</sup> )	$I_{corr}$ ( $\mu A cm^{-2}$ )	$\eta_{Tafel}$ (%)
HCl	1	475.9	175.6	1077.8	-
PPIB1	$10^{-2}$	472.1	167.7	130.5	87.9
	$10^{-3}$	481.6	164.7	162.0	85.0
	$10^{-4}$	476.9	170.4	283.8	73.7
	$10^{-5}$	490.4	192.6	455.4	57.7
	$10^{-2}$	474.4	171.5	063.9	94.1
	$10^{-3}$	471.8	187.9	168.0	84.4
PPIB4	$10^{-4}$	472.0	167.7	215.9	79.9
	$10^{-5}$	504.2	196.4	353.0	67.2

### 3.3. Electrochemical impedance spectroscopy (EIS) studies

Nyquist representations of different inhibitors are shown in Figs 7 and 8. It is clear from all plots that impedance response of carbon steel in test solution was significantly changed after adding the inhibitors. The several theoretical circuits were applied for the study the impedance behavior. The standard Randle circuit (Fig 9) was mostly fit in the present studies that have impedance spectra containing single capacitive semicircle. The circuit composed of uncompensated solution resistance ( $R_s$ ), charge transfer resistance ( $R_{ct}$ ), double layer capacitance ( $C_{dl}$ ). Various parameters such as charge transfer resistance ( $R_{ct}$ ), double layer capacitance ( $C_{dl}$ ) and percentage inhibition efficiency ( $\eta_z(\%)$ ) have been calculated and listed in Table 7. The existence of single semi circle showed the single charge transfer process during dissolution which is unaffected by the presence of inhibitor molecule. Increasing of the charge transfer resistance and decreasing of the double layer capacitance with

increasing the inhibitor concentration indicated that these compounds inhibited the corrosion rate of carbon steel by an adsorption mechanism [57]. In fact, the presence of both compounds increased the value of the charge transfer resistance in the acidic solution. The effect being most pronounced with the PPIB4. The increment in charge transfer resistance value is attributed to the formation of protective film on the metal/solution interface [58, 59]. The values of  $C_{dl}$  of studied compounds decreased with increasing the concentrations. The decrease in  $C_{dl}$  is attributed to increase in the thickness of electronic double layer [60]. The decrease in the values of  $C_{dl}$  follows the order similar to that obtained for the  $I_{corr}$  studies. This can be explained on the basis of adsorption of imidazolium derivatives on the metal surface [61].

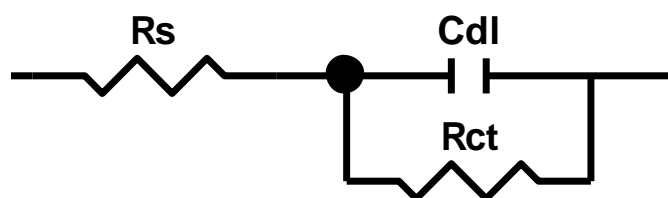


**Figure 9.** Equivalent circuit model for the carbon steel/hydrochloric acid electrolyte.

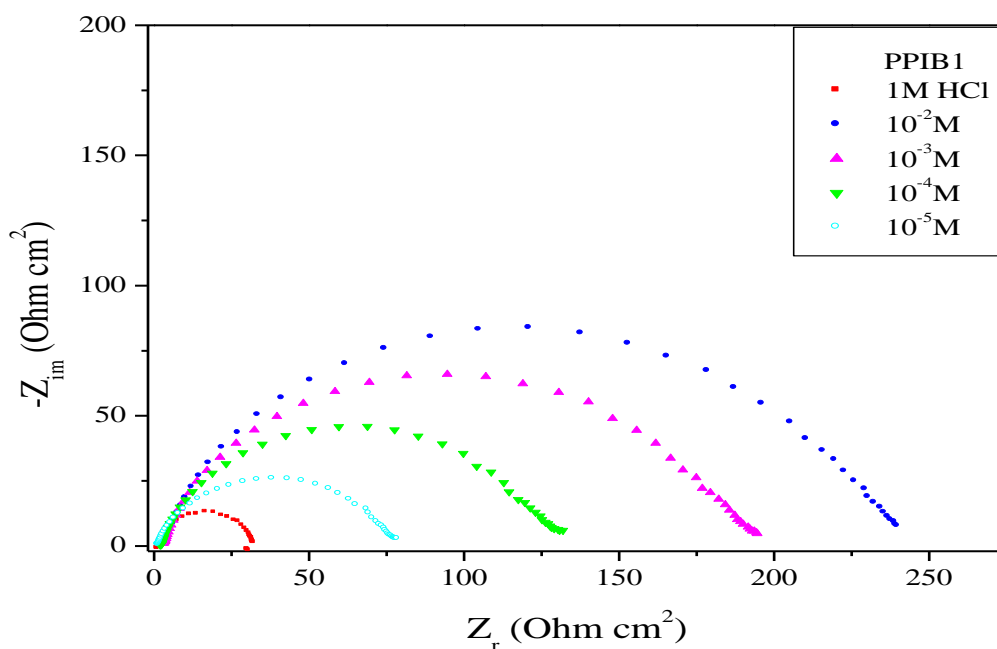


**Figure 7.** Nyquist diagrams for carbon steel in 1.0 M HCl containing different concentrations of PPIB1 at 308 K.

$C_{dl}$  values were calculated from the frequency at which the imaginary component of impedance was maximum ( $Z_{im, max}$ ) using the following relation:

$$C_{dl} = \frac{1}{2\pi f_{max} R_{ct}} \tag{8}$$

The percentage  $\eta_Z(\%)$  was calculated using the following equation:

$$\eta_Z(\%) = \frac{R_{ct(i)} - R_{ct}}{R_{ct(i)}} \times 100 \tag{9}$$

Where  $R_{ct}$  and  $R_{ct(i)}$  are the charge-transfer resistance values without and with inhibitor respectively.

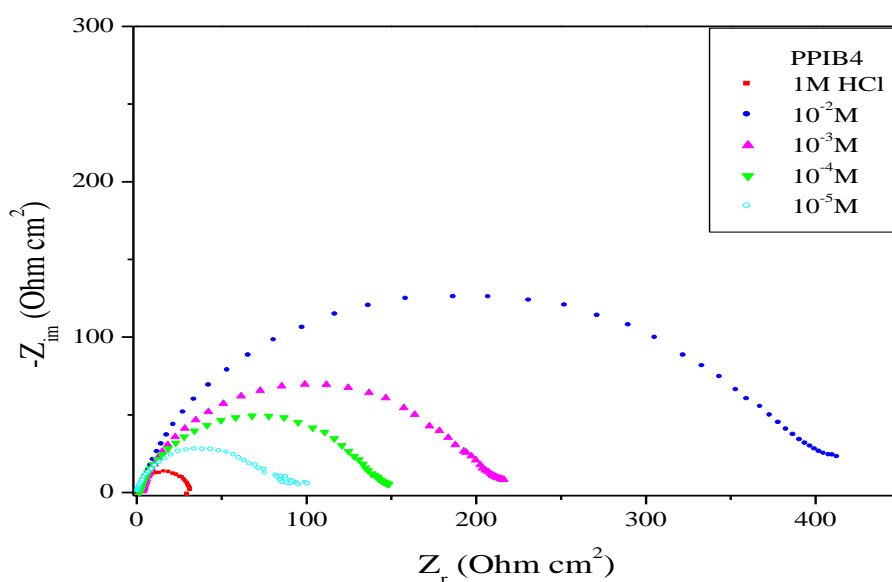


**Figure 8.** Nyquist diagrams for carbon steel in 1.0 M HCl containing different concentrations of PPIB4 at 308 K.

**Table 7.** Electrochemical impedance parameters for carbon steel in 1.0 M HCl in absence and presence different concentrations of inhibitors

Inhibitors	Conc (M)	$R_{ct}$ ( $\Omega.cm^2$ )	$f_{max}$ (Hz)	$C_{dl}$ ( $\mu F/cm^2$ )	$\eta_Z$ (%)
HCl	1	031.0	63.34	80.99	-
PPIB1	$10^{-2}$	242.5	15.78	41.46	87.2
	$10^{-3}$	195.3	20.00	40.76	84.1
	$10^{-4}$	129.5	25.00	49.18	76.0
	$10^{-5}$	077.6	40.00	51.30	60.0
PPIB4	$10^{-2}$	418.8	12.50	30.42	92.6
	$10^{-3}$	212.7	20.00	37.43	85.4
	$10^{-4}$	146.0	40.00	43.63	78.7
	$10^{-5}$	095.5	40.00	41.68	67.5

The results obtained from the EIS technique in 1.0 M HCl solution were in good agreement with those obtained from weight loss method and potentiodynamic polarization method.

#### 4. CONCLUSION

Eco-friendly ionic liquids PPIB1 and PPIB4 have been successfully synthesized utilizing MW method with chemical yields of 85% and 88%, respectively. These new ionic liquids have potential as corrosion inhibitor. Inhibition efficiency increases with increasing inhibitor concentration. Polarization curves proved that PPIB1 and PPIB4 are a mixed-type inhibitor, which can suppress anodic and cathodic reactions at the same time. EIS plots indicated that the inhibitor increases the charge-transfer resistances and showed that the inhibitive performance depends on adsorption of the molecules on the metal surface. The adsorption of PPIB1 and PPIB4 on carbon steel surface was found to obey the Langmuir adsorption isotherm. The negative values of  $\Delta G_{ads}^{\circ}$  indicated a spontaneous adsorption of the inhibitor on the surface of steel. The inhibition efficiencies were determined using the polarization and EIS plots, which were in good agreement with the weight loss measurements.

#### ACKNOWLEDGEMENTS

Prof S. S. Al-Deyab and Prof B. Hammouti extend their appreciation to the Deanship of Scientific Research at King Saud University for funding the work through the research group project.

#### References

1. H. Keles, M. Keles, I. Dehri, O. Serindag, *Mater. Chem. Phys.* 112 (2008) 173.
2. H. Wang, H. Fan, J. Zheng, *Mater. Chem. Phys.* 77 (2003) 655.
3. S.A.A. El-Maksoud, A.S. Fouda, *Mater. Chem. Phys.* 93 (2005) 84.
4. M. Lagrenee, B. Mernari, M. Bouanis, M. Traisnel, F. Bentiss, *Corros. Sci.* 44 (2002) 573.
5. M. Abdallah, *Corros. Sci.* 45 (2003) 2705.
6. I.B. Obot, N.O. Obi-Egbedi, *Corros. Sci.* 52 (2010) 657.
7. H. Zarrok, S. S. Al-Deyab, A. Zarrouk, R. Salghi, B. Hammouti, H. Oudda, M. Bouachrine, F. Bentiss, *Int. J. Electrochem. Sci.* 7 (2012) 4047.
8. H. Zarrok, H. Oudda, A. El Midaoui, A. Zarrouk, B. Hammouti, M. Ebn Touhami, A. Attayibat, S. Radi, R. Touzani, *Res. Chem. Intermed.* (2012) DOI: 10.1007/s11164-012-0525-x).
9. H. Zarrok, R. Salghi, A. Zarrouk, B. Hammouti, H. Oudda, Lh. Bazzi, L. Bammou, S. S. Al-Deyab, *Der Pharm. Chem.* 4 (2012) 407.
10. A. Ghazoui, R. Saddik, N. Benchat, B. Hammouti, M. Guenbour, A. Zarrouk, M. Ramdani, *Der Pharm. Chem.* 4 (2012) 352.
11. A. Zarrouk, B. Hammouti, H. Zarrok, R. Salghi, A. Dafali, Lh. Bazzi, L. Bammou, S. S. Al-Deyab, *Der Pharm. Chem.* 4 (2012) 337.
12. H. Zarrok, H. Oudda, A. Zarrouk, R. Salghi, B. Hammouti, M. Bouachrine, *Der Pharm. Chem.* 3 (2011) 576.
13. Z. Hua, S.Q. Xia, P.S. Ma, *Chem. Technol. Biotechnol.* 80 (2005) 1089.
14. M.A.M. Ibrahim and M. Messali, *Products Finishing.* 76 (2011) 14.
15. F. Endres, *Chem. Phys. Chem.* 3 (2002) 144.

16. T. Sato, T. Maruo, S. Marukane, K. Takagi, *J. Power Source*. 138 (2004) 253.
17. M. Ue, M. Takeda, A. Toriumi, A. Kominato, R. Hagiwara, Y. Ito, *J. Electrochem. Soc.* 150 (2003) 499.
18. R. Gasparac, C.R. Martin, E. Stupnisek-Lisac, *J. Electrochem. Soc.* 147 (2000) 548.
19. D.Q. Zhang, L.X. Gao, G.D. Zhu, *Corros. Sci.* 46 (2004) 3031.
20. S. Muralidharan, S.V.K. Iyer, *Anti-Corros. Met. Mater.* 44 (1997) 100.
21. M.A.M. Ibrahim, M. Messali, Z. Moussa, A. Y. Alzahrani, S. N. Alamry, B. Hammouti, *Port. Electrochim. Acta.* 29 (2011) 375.
22. M. Messali, *J. Mater. Environ. Sci.* 2 (2011) 174.
23. P. T. Anastas, Warner, *Green Chemistry, Theory and Practice*, Oxford University Press, Oxford, UK, 1998.
24. A. C. R. Loupy, *Chimie.* 7 (2004) 103.
25. A. Aupoix, B. Pegot, G. Vo-Thanh, *Tetrahedron.* 66 (2010) 1352.
26. F. Yi, Y. Peng, G. Song, *Tetrahedron Lett.* 46 (2005) 3931.
27. V. Singh, S. Kaur, V. Sapehiya, J. Singh, G. L. Kad, *Catalysis Comm.* 6 (2005) 57.
28. M. Messali and S. A. Ahmed, *Green and Sustainable Chemistry.* 1 (2011) 70.
29. M. Messali, *Arabian Journal of Chemistry.* (2011) doi:10.1016/j.arabjc.2011.06.030.
30. I. Ahamad, R. Prasad, M.A. Quraishi, *Corros. Sci.* 52 (2010) 933.
31. F. Bentiss, M. Outirite, M. Traisnel, H. Vezin, M. Lagrenée, B. Hammouti, S.S. Al-Deyab, C. Jama, *Int. J. Electrochem. Sci.* 7 (2012) 1699.
32. M. Lagrenée, B. Mernari, M. Bouanis, M. Traisnel, F. Bentiss, *Corros. Sci.* 44 (2002) 573.
33. A.S. Fouda, M.N. Moussa, F.I.M. Taha, A.I. Elneanaa, *Corros. Sci.* 26 (1986) 719.
34. S.M. Hassan, M.N. Moussa, F.I.M. Taha, A.S. Fouda, *Corros. Sci.* 21 (1981) 439.
35. M.A. Quraishi, M.A.W. Khan, M. Ajmal, S. Muralidharan, S.V. Iyer, *Br. Corros. J.* 32 (1997) 72.
36. F.Z. Bouanis, F. Bentiss, M. Traisnel, C. Jama, *Electrochim. Acta.* 54 (2009) 2371.
37. O.L. Riggs, R.M. Hurd, *Corrosion.* 23 (1967) 252.
38. A.S. Fouda, A.A. Al-Sarawy, E.E. El-Katori, *Desalination.* 201 (2006) 1.
39. T. Szauer, A. Brand, *Electrochim. Acta.* 26 (1981) 1219.
40. R. Solmaz, G. Kardas\_, M. Culha, B. Yazıcı, M. Erbil, *Electrochim. Acta.* 53 (2008) 5941.
41. R. Solmaz, G. Kardas\_, B. Yazıcı, M. Erbil, *Colloids Surf. A Physicochem. Eng. Aspects.* 312 (2008) 7.
42. N.M. Guan, L. Xueming, L. Fei, *Mater. Chem. Phys.* 86 (2004) 59.
43. I. El Ouali, B. Hammouti, A. Aouniti, Y. Ramli, M. Azougagh, E.M., Essassi and M. Bouachrine, *J. Mater. Environ. Sci.* 1 (2010) 1.
44. E. Bayol, K. Kayakırılmaz, M. Erbil, *Mater. Chem. Phys.* 104 (2007) 74.
45. S.A. Ali, M.T. Saeed, S.U. Rahman, *Corros. Sci.* 45 (2003) 253.
46. J. Flis, T. Zakroczyński, *J. Electrochem. Soc.* 143 (1996) 2458.
47. G. Avci, *Mater. Chem. Phys.* 112 (2008) 234.
48. E. Bayol, A.A. Gurten, M. Dursun, K. Kayakırılmaz, *Acta Phys. Chim. Sin.* 24 (2008) 2236.
49. O.K. Abiola, N.C. Oforka, *Mater. Chem. Phys.* 83 (2004) 315.
50. M. Ozcan, R. Solmaz, G. Kardas, I. Dehri, *Colloid Surf. A.* 325 (2008) 57.
51. F. Hongbo, "Synthesis and application of new type inhibitors", Chemical Industry Press, Beijing, (2002) p.166.
52. S.A. Ali, H.A. Al-Muallem, M.T. Saeed, S.U. Rahman, *Corros. Sci.* 50 (2008) 664.
53. M. Lebrini, F. Bentiss, N. Chihib, C. Jama, J.P. Hornez, M. Lagrenée, *Corros. Sci.* 50 (2008) 2914.
54. E. McCafferty, *Corros. Sci.* 47 (2005) 3202.
55. M. Bouklah, N. Benchat, A. Aouniti, B. Hammouti, M. Benkaddour, M. Lagrenée, H. Vezin, F. Bentiss, *Prog. Org. Coat.* 51 (2004) 118.
56. I. Ahamad, M.A. Quraishi, *Corros. Sci.* 52 (2010) 651.
57. M.A. Quraishi, J. Rawat, *Mater. Chem. Phys.* 70 (2001) 95.

58. A.K. Singh, M.A. Quraishi, *Corros. Sci.* 53 (2011) 1288.
59. S. Murlidharan, K.L.N. Phani, S. Pitchumani, S. Ravichandran, *J. Electrochem. Soc.* 142 (1995) 478.
60. M.G. Hosseini, M. Ehteshamzadeh, T. Shahrabi, *Electrochem. Acta* 52 (2007) 3680.
61. A.K. Singh, M.A. Quraishi, *J. Appl. Electrochem.* 41 (2011) 7.